第五章:

大气环流中的纬向环流系统

5.1 Storm Tracks

授课教师：张洋

2019. 11. 17

Zonally averaged meridional circulations

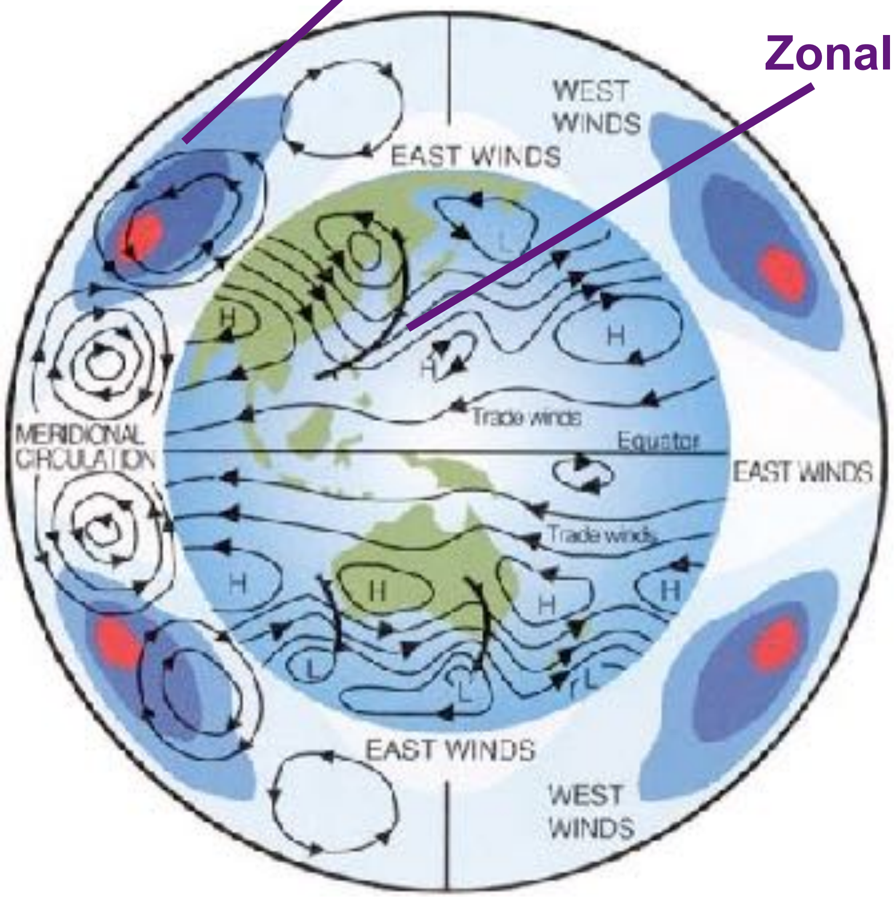

Zonal asymmetry

- 经向环流系统（纬向平均环流, zonally averaged circulations）：
  - Hadley 环流
  - Ferrel 环流、急流、波流相互作用
- 纬向环流系统（non-zonal circulations）：
  - Storm tracks
  - Monsoon
  - ENSO and Walker circulation
- 不同复杂度的大气环流模式
- 全球变暖背景下的大气环流

Non-zonal circulations

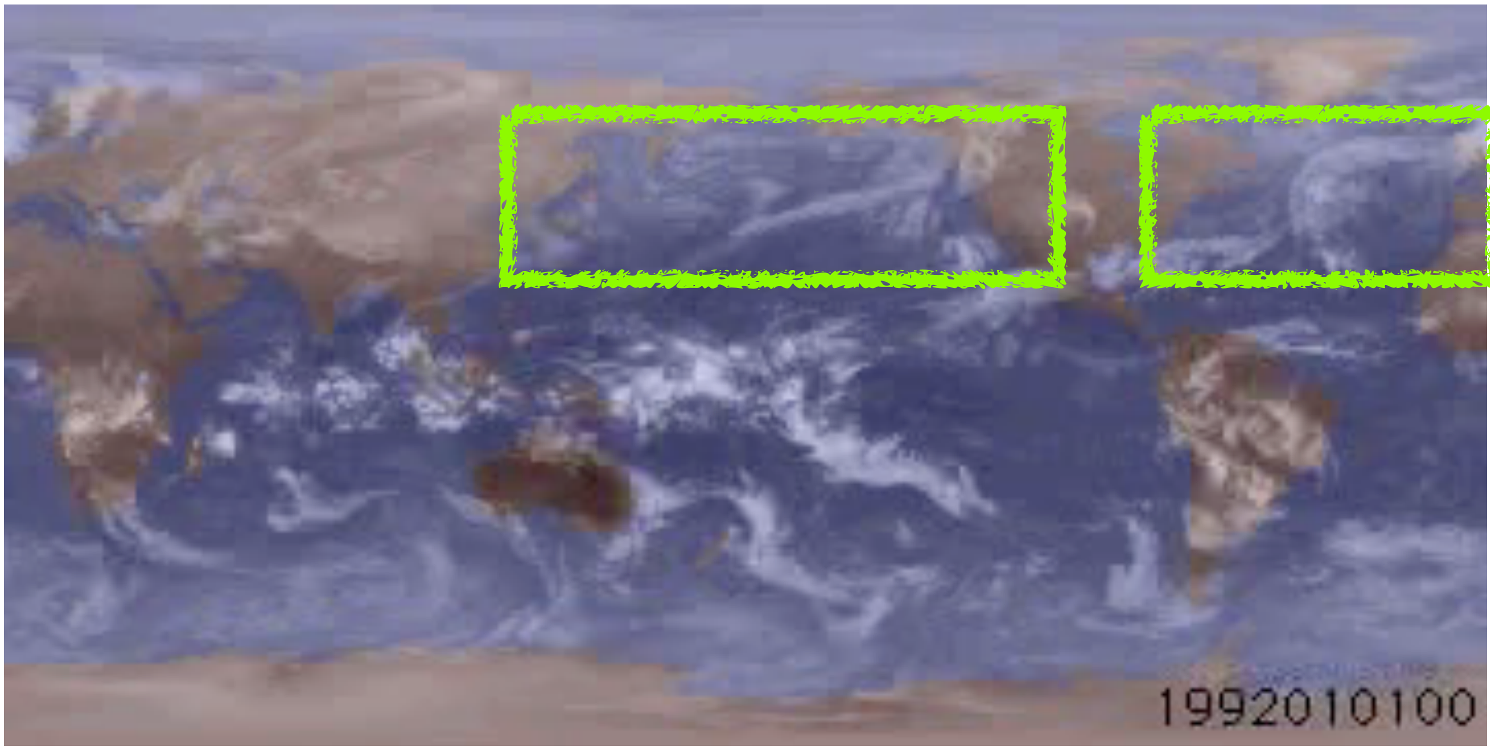

Outline

- Observed features
  - from two basic approaches
  - seasonal variation
  - inter-annual, decadal variations
- Storm track dynamics
  - Baroclinic eddy life cycle
  - Transient eddy energy budget
- Summary and discussion

Observed features

- Two basic approaches to diagnosing storm tracks:
  - The traditional one: track the position of individual weather systems, produce statistics for their distributions, e.g. track densities, storm life span...
  - The bandpass filtering approach (in synoptic time scales): estimate the statistics at a set grid points in analyzed fields, which can provide a 3-d picture of storm tracks.

Observed features

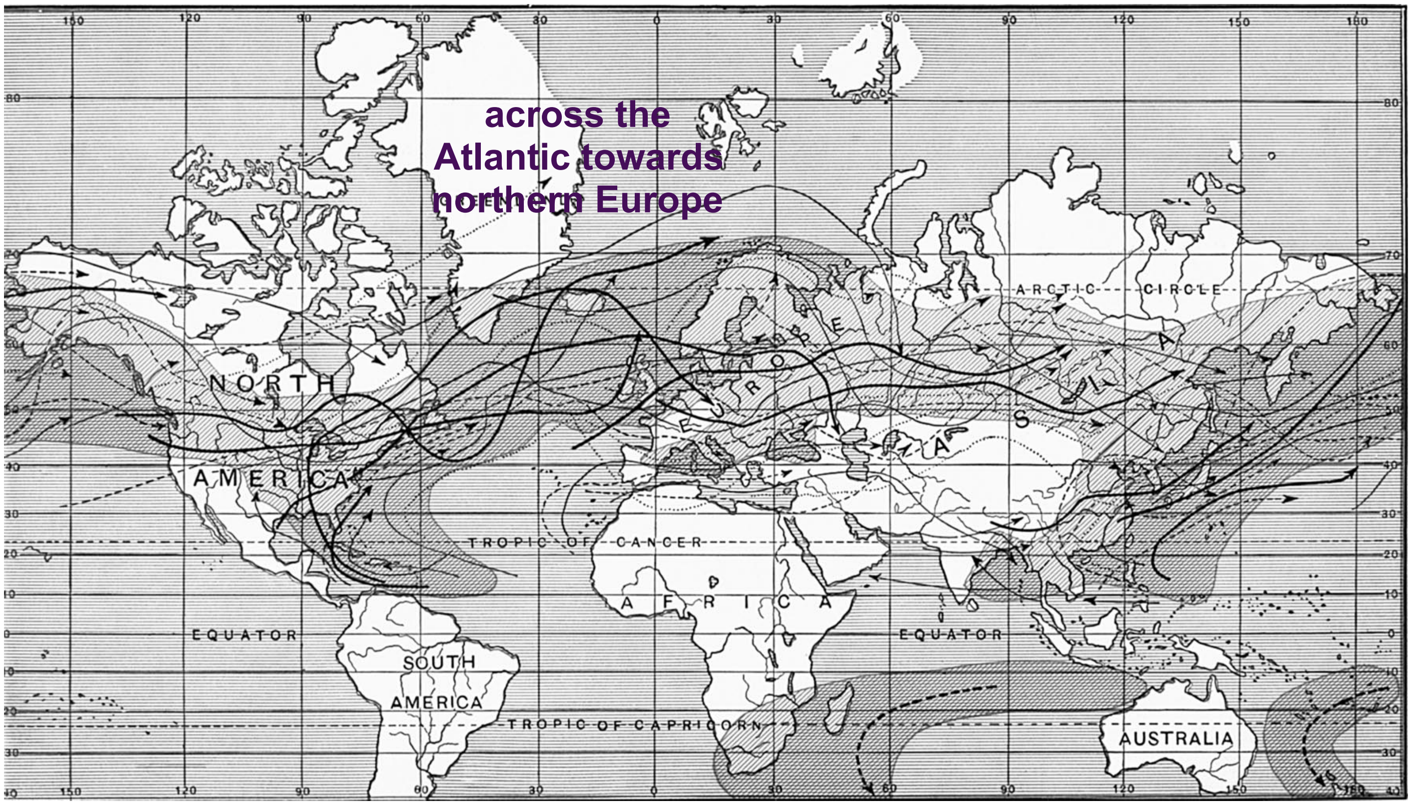

from the East China sea across the Pacific

FIG. 1. A figure from an 1888 geography text showing storm frequency distribution as viewed in the mid-nineteenth century. The stipling denotes high storm frequency, while the arrows indicate individual storms. Reproduced from Hinman (1888).

Observed features

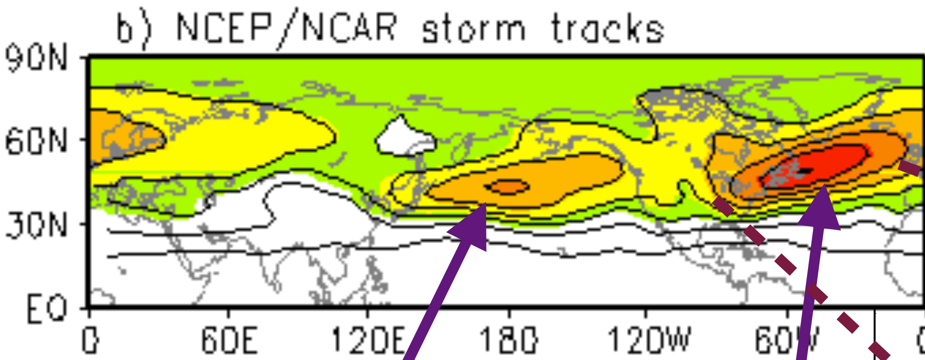

Shaded: standard deviation of 24-h filtered 500-hPa geopotential height (contour interval 20 m) computed from the Januaries of 1982-1994 (NCEP/NCAR reanalysis)
(From Chang's homepage)

Two storm track zones in N.H.

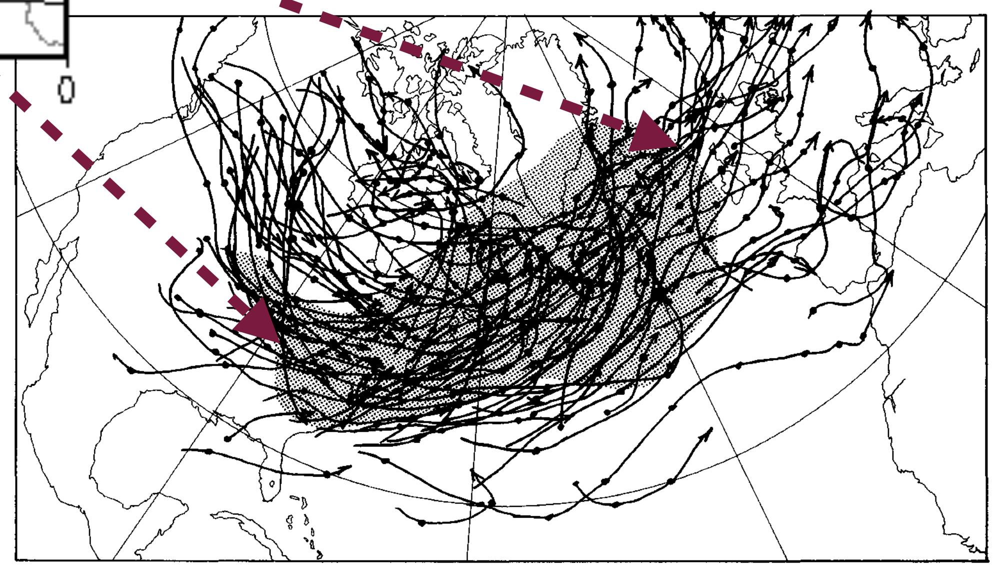

Fig. 7.9. The tracks of low pressure centres over the North Atlantic for the period December 1985 to February 1986. The shading indicates the region where the high frequency $\overline{Z'^2}^{1/2}$ exceeded 90 m in the ECMWF analyses for the same period.

Observed features

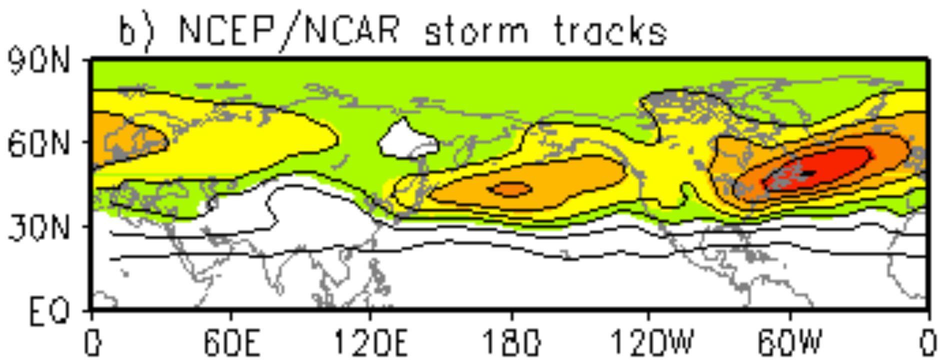

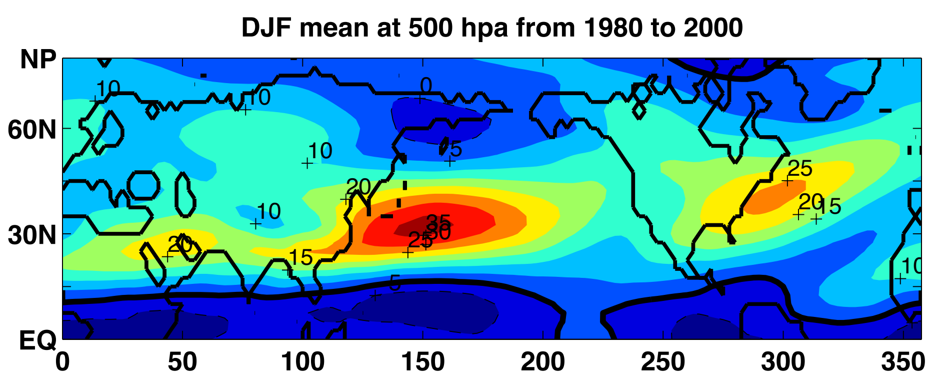

Zonal wind from NCEP/NCAR data

The storm zones occur in association with the jet streams;

The storm zones are most intense near the longitude of the jet exits.

Observed features

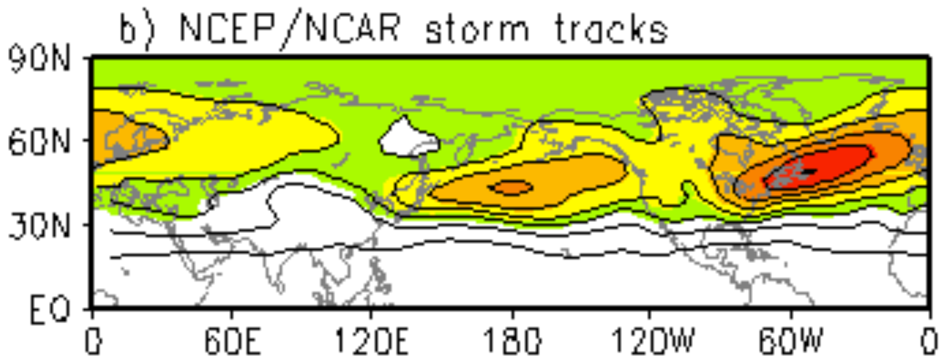

Temperature distribution from NCEP/NCAR data

DJF mean at 850 hpa from 1980 to 2000

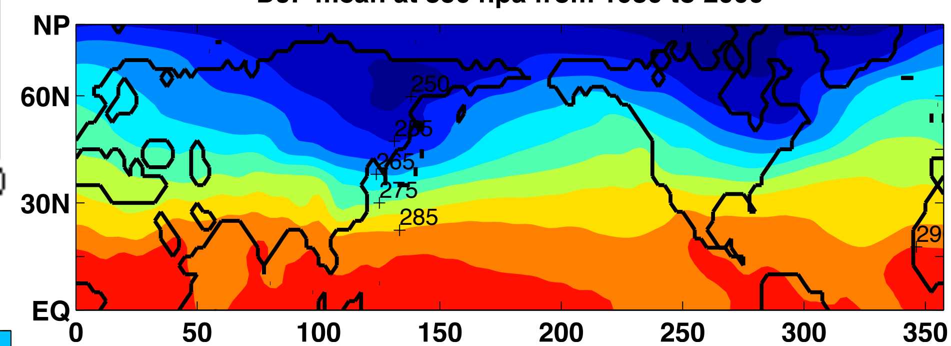

DJF mean at 500 hpa from 1980 to 2000

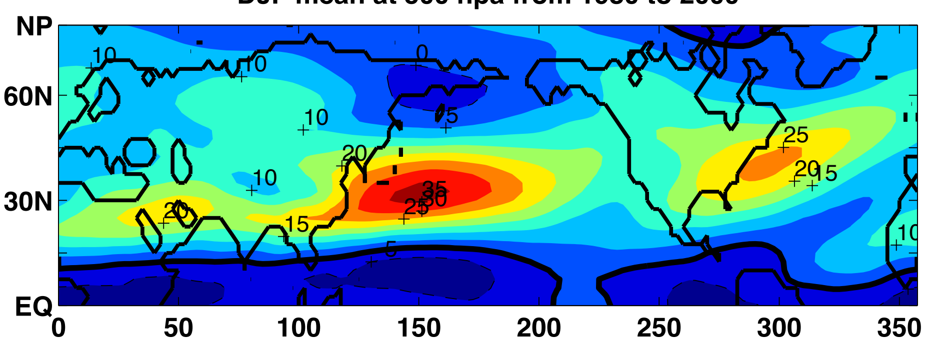

Zonal wind from NCEP/NCAR data

DJF mean at 500 hpa from 1980 to 2000

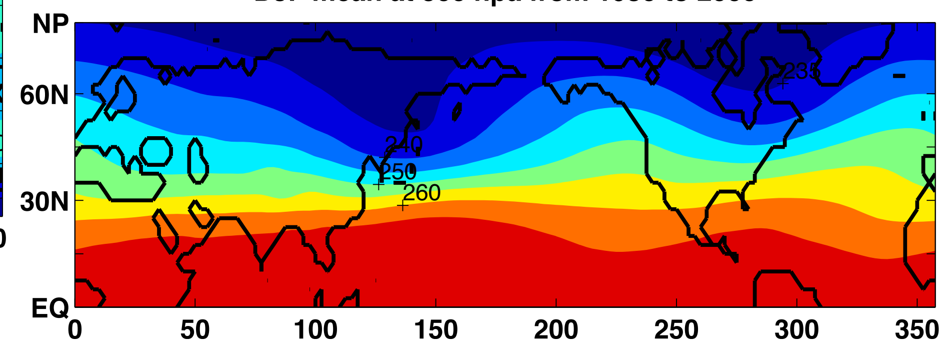

Observed features

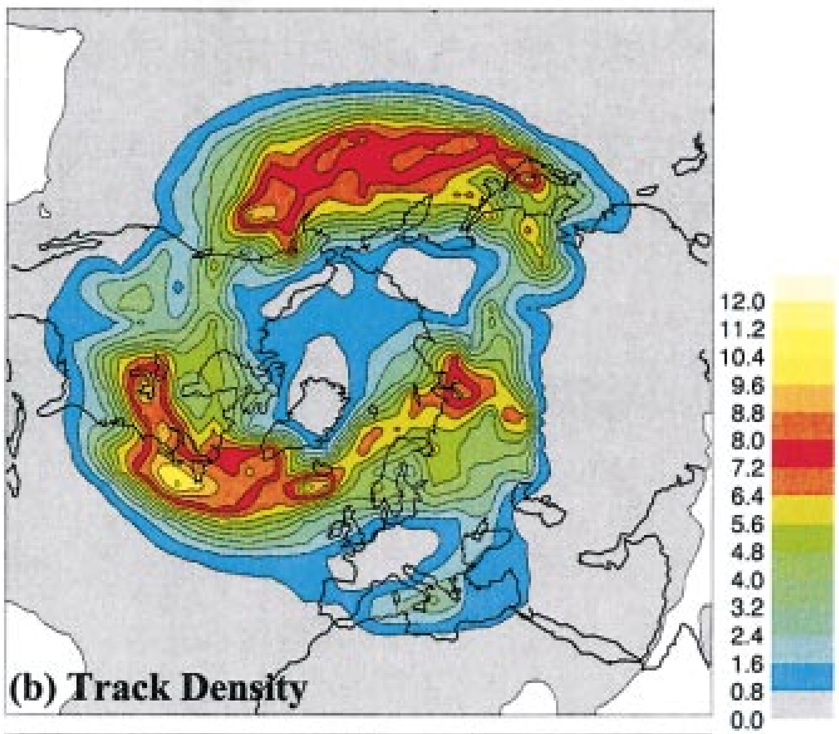

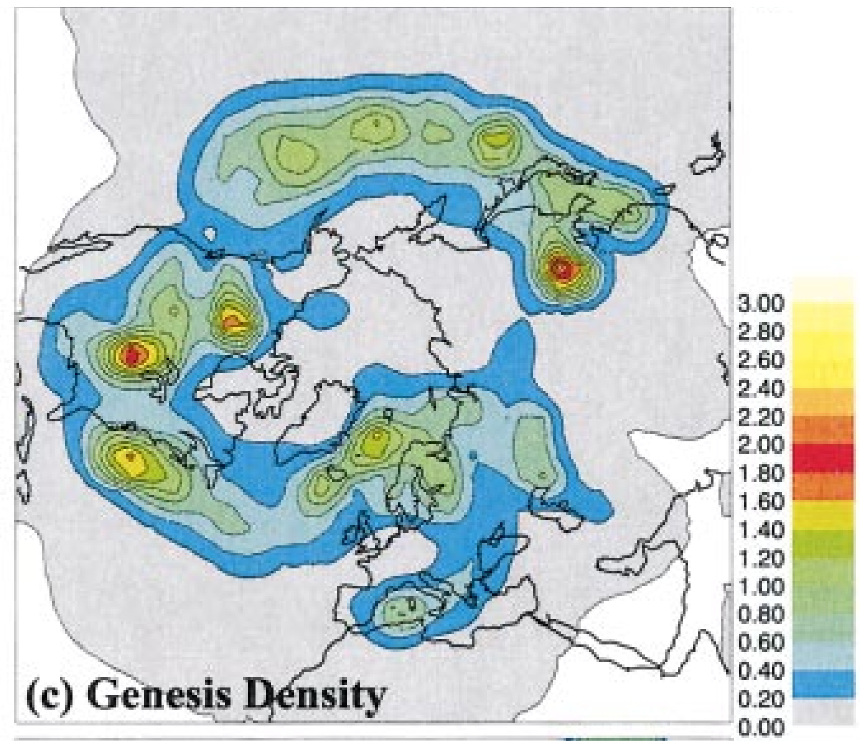

Using ECMWF, MSLP,
from Hoskins and Hodges, 2002

Observed features

$$\sigma = kc_i \approx 0.3\,\Lambda \frac{f_o}{N}$$

Eddy kinetic energy

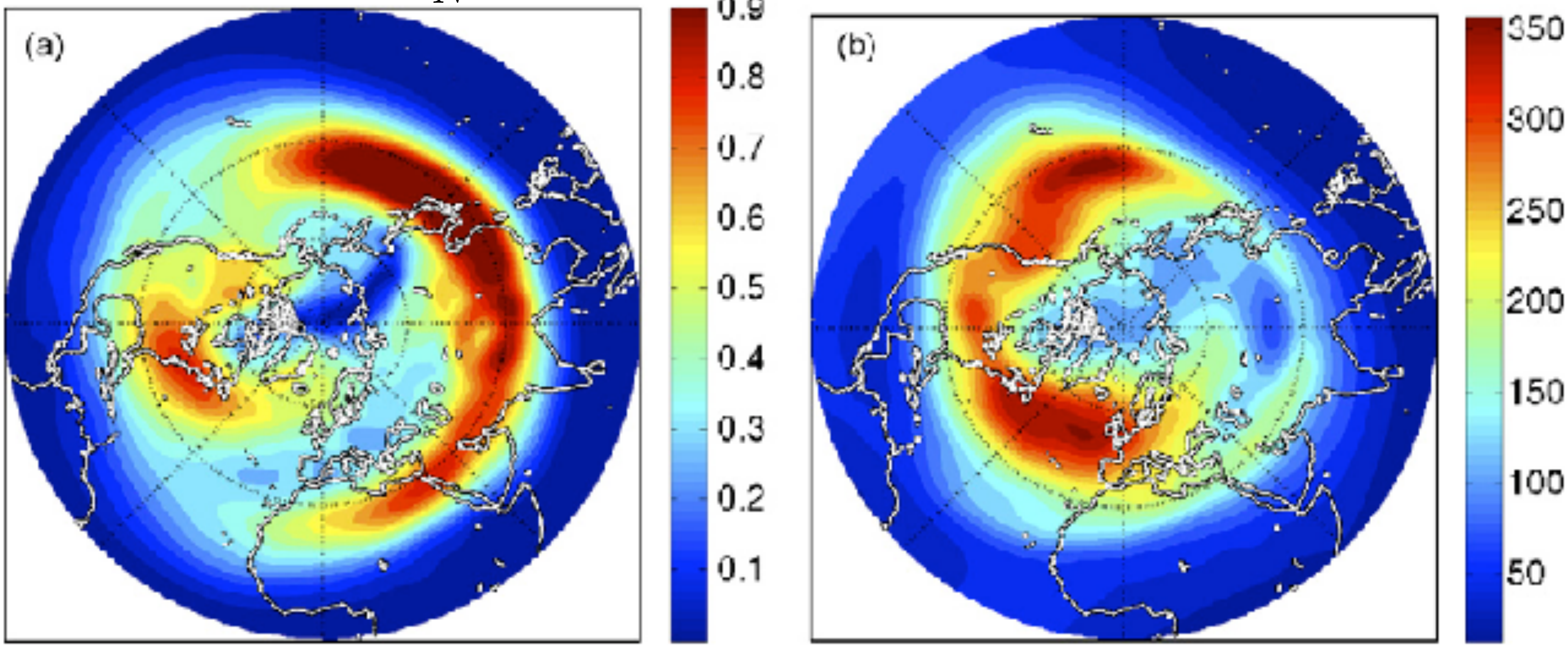

Fig. 2. Left: the Eady growth rate, σ_E, at 500 hPa in units of 1/days. Right: The average eddy kinetic energy at 250 hPa in units of $(m/s)^2$. Both are for the Northern Hemisphere winter (DJF), computed from the NCEP/NCAR re-analysis. The maxima in EKE are downstream of the maxima in growth rate, and the Pacific storm track does not fully decay before the beginning of the Atlantic storm track. The prime meridian (Greenwich) is at 6 O'clock.

from Vallis and Gerber, 2008

Observed features

eddy momentum flux

eddy heat flux

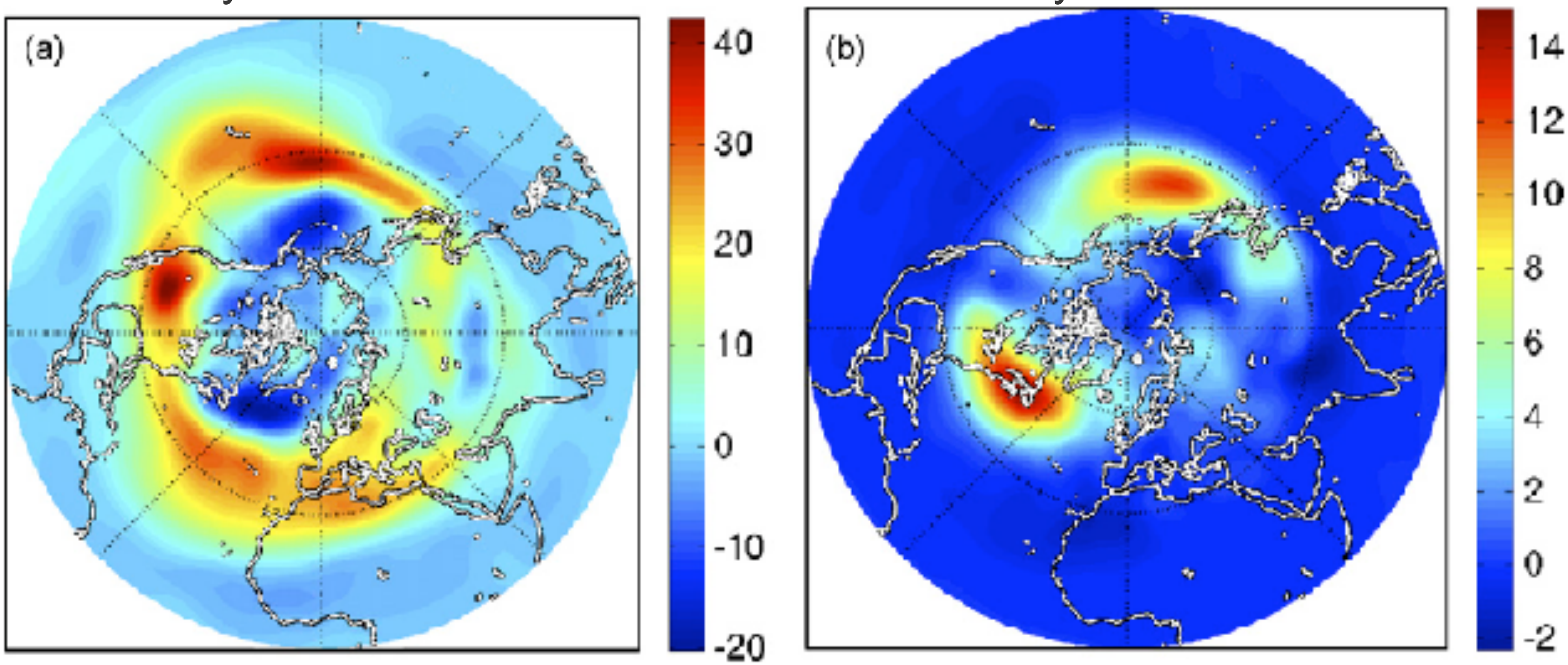

Fig. 3. Left: the eddy momentum fluxes at 250 hPa $(m/s)^2$. Right: the eddy heat fluxes at 500 hPa (mK/s), for the Northern Hemisphere winter (DJF). Both sets of data are band-pass filtered, allowing variability from 2 to 10 days, from the NCEP/NCAR re-analysis. Red values are large, blue values weak or negative.

from Vallis and Gerber, 2008

Observed features

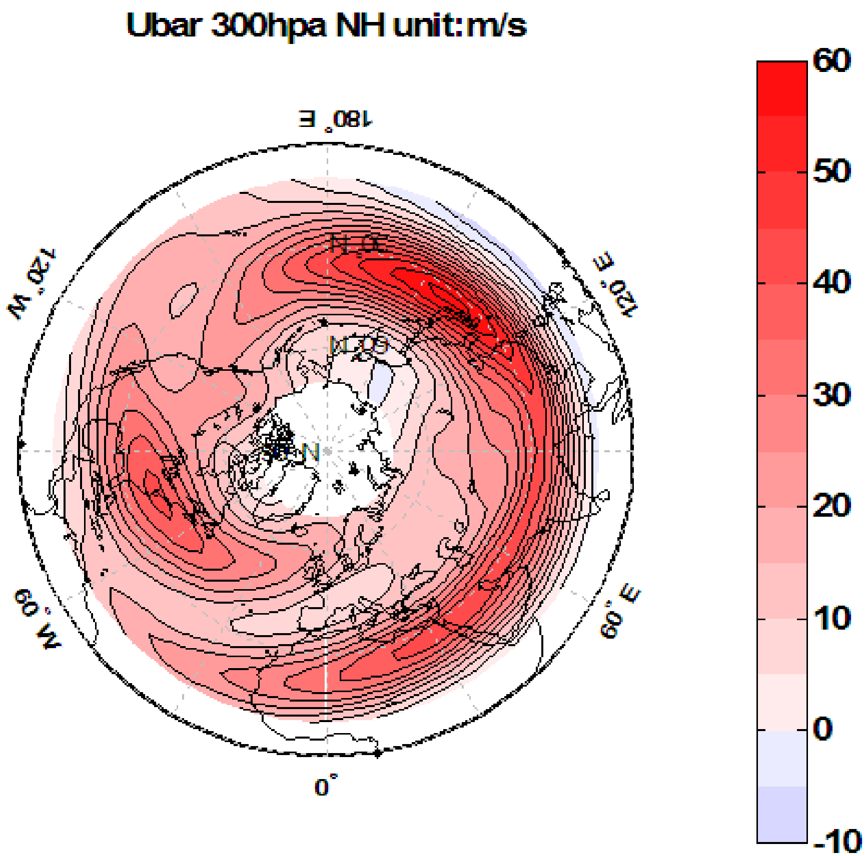

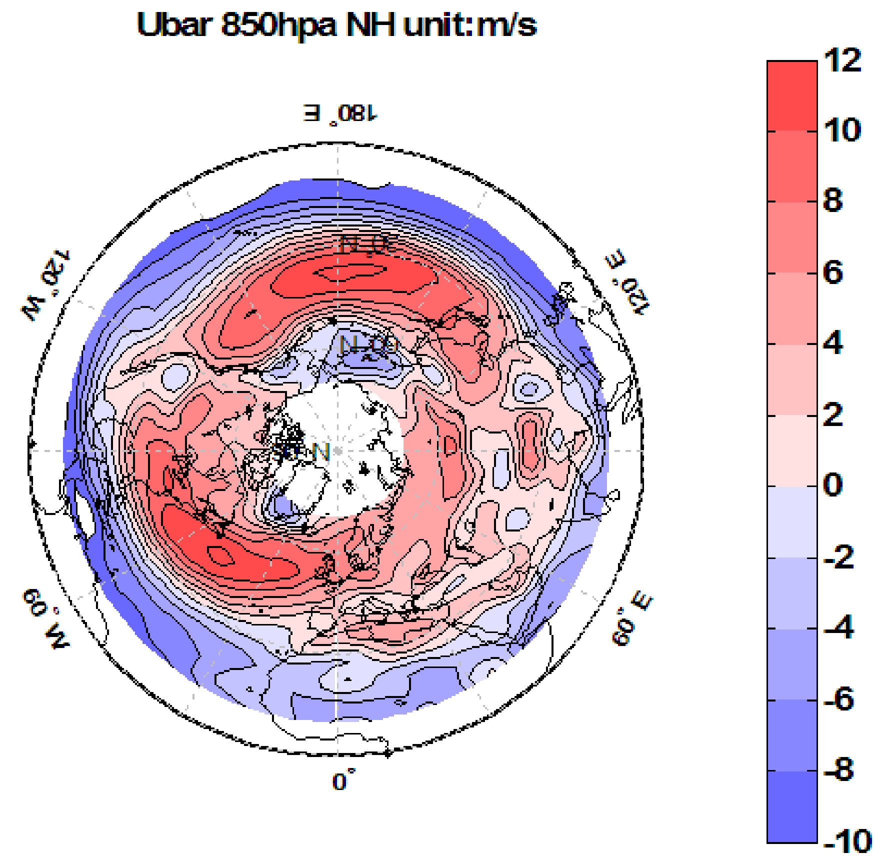

From Dai Ying, 2011

Observed features

a.大西洋地区配置关系示意图

b. 太平洋地区

（1）交换上图中300hpa瞬变动能大值和动量通量大值位置；

（2）水平方向两两之间距离增大。

From Dai Ying, 2011

Beyond the zonal average: Zonal variation

- Transient eddy transport of vq:

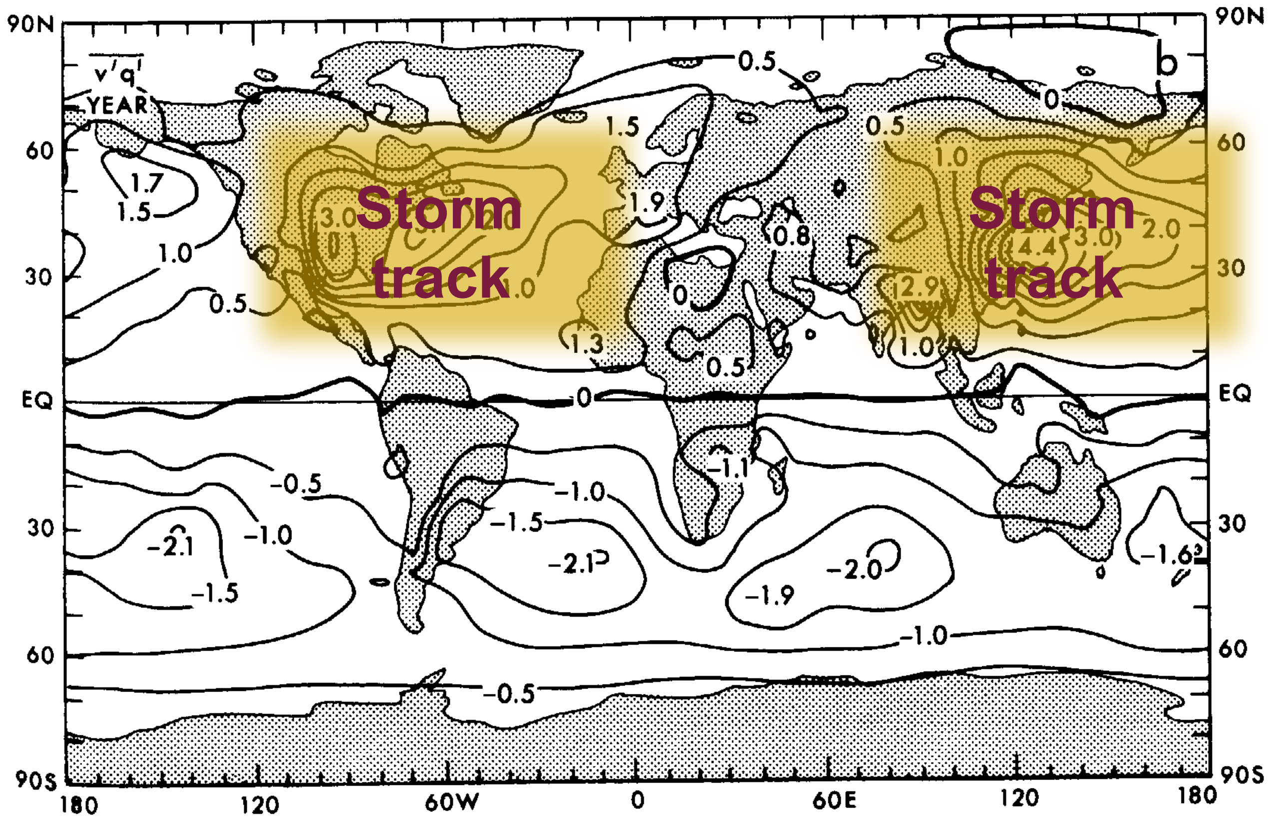

Strongest over the western coast of oceans in the midlatitudes of the Northern Hemisphere

Observed features

- Seasonal variation

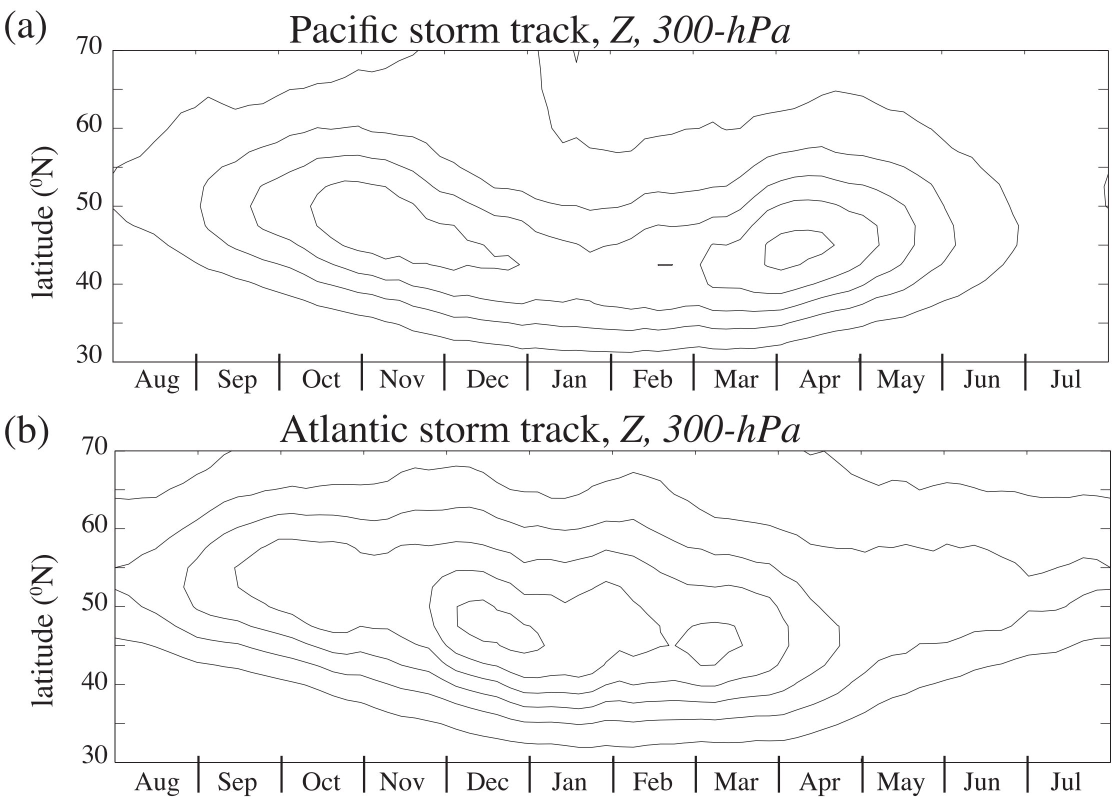

FIG. 1. Midwinter suppression of the Pacific storm track, shown as the variance in geopotential height at 300 hPa: (a) Pacific domain (20°–70°N, 140°E–180°) and (b) Atlantic domain (20°–70°N, 30°–70°W). The contour interval is 1500 m^2 starting at 2000 m^2. This is an update of Fig. 2 in Nakamura (1992) for the ERA-40 dataset between 1958 and 2001. The data are 2–6 day bandpass filtered using a fourth-order Butterworth filter to obtain daily climatologies. Results are smoothed with a 31-day running mean filter and plotted every five days. Large tick marks on the abscissa correspond to the first day of each month.

Most intense in the transition seasons, MAM and SON, weaker in DJF (**mid-winter minimum**), whose variation is not consistent with the mean flow baroclinicity.

Strongest in DJF and least pronounced in JJA, with the actual position varies little

Observed features

- Seasonal variation

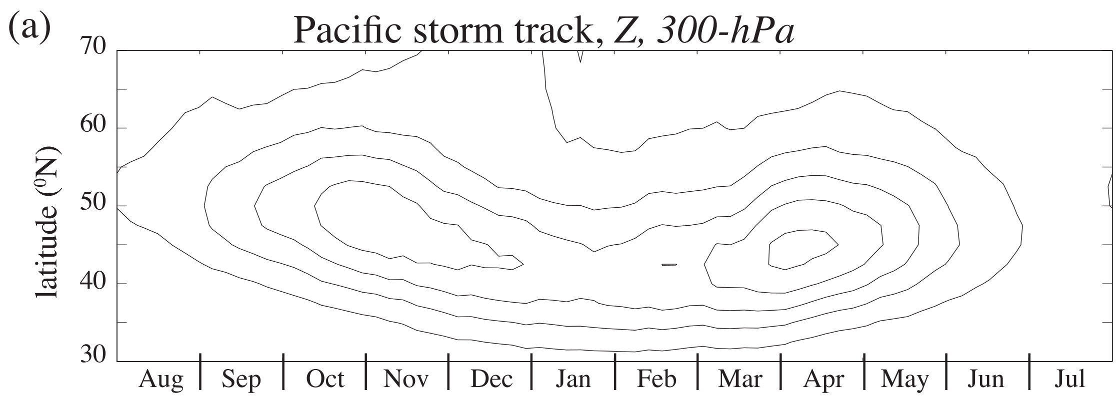

Most intense in the transition seasons, MAM and SON, weaker in DJF (**mid-winter minimum**), whose variation is not consistent with the mean flow baroclinicity.

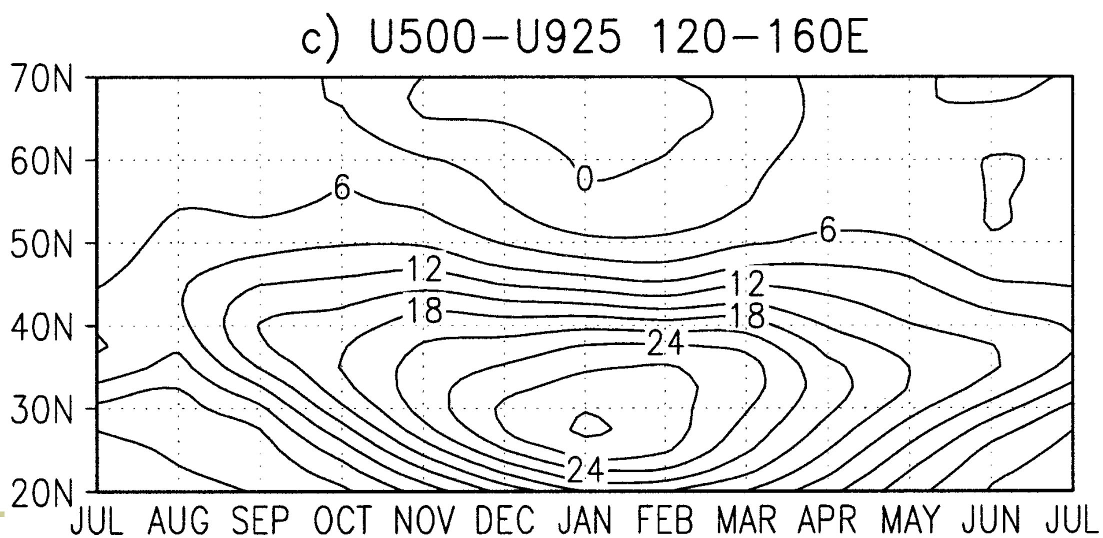

Mean flow baroclinic zone moves equatorward and becomes strongest in winter.

Observed features

- Seasonal variation

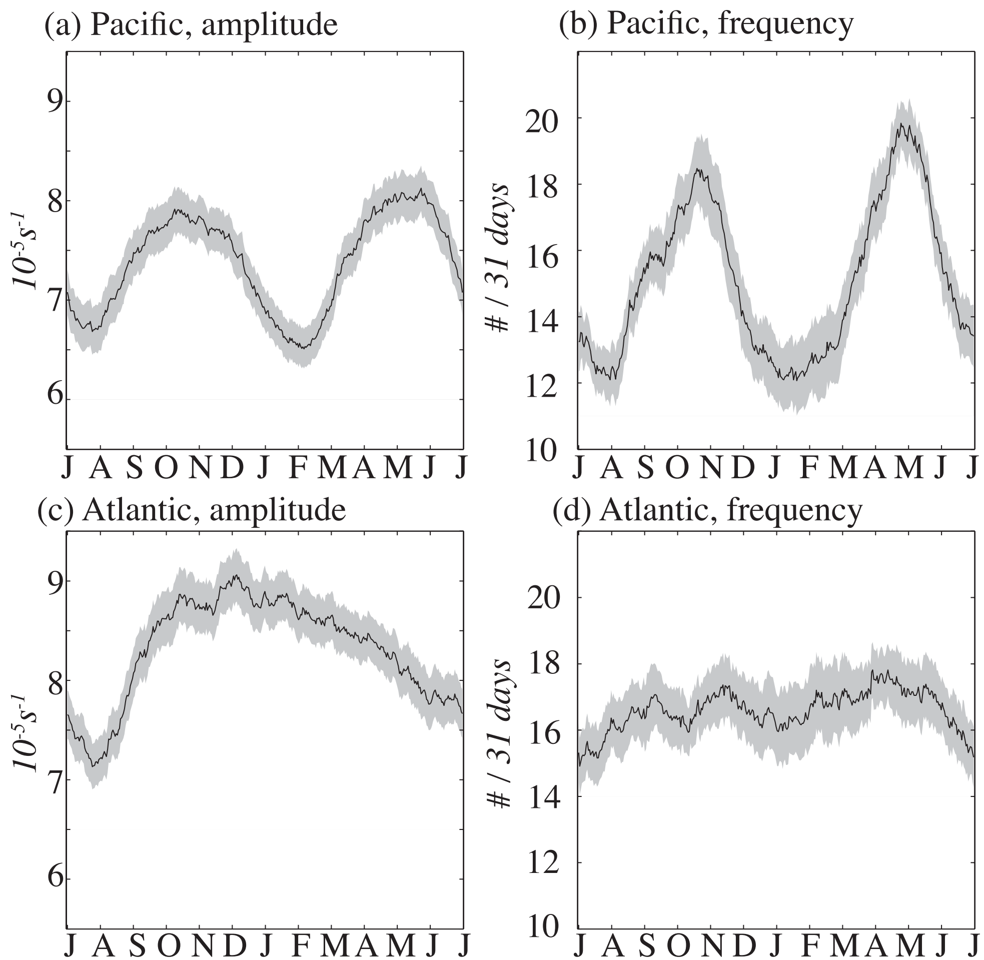

FIG. A1. As in Fig. 3 but for relative vorticity at 300 hPa. Units in (a) and (c) are 10^{-5} s^{-1}.

Different seasonalities between the Pacific and Atlantic storm tracks.

from Penny et al, JC, 2010

Observed features

- Inter-annual variation

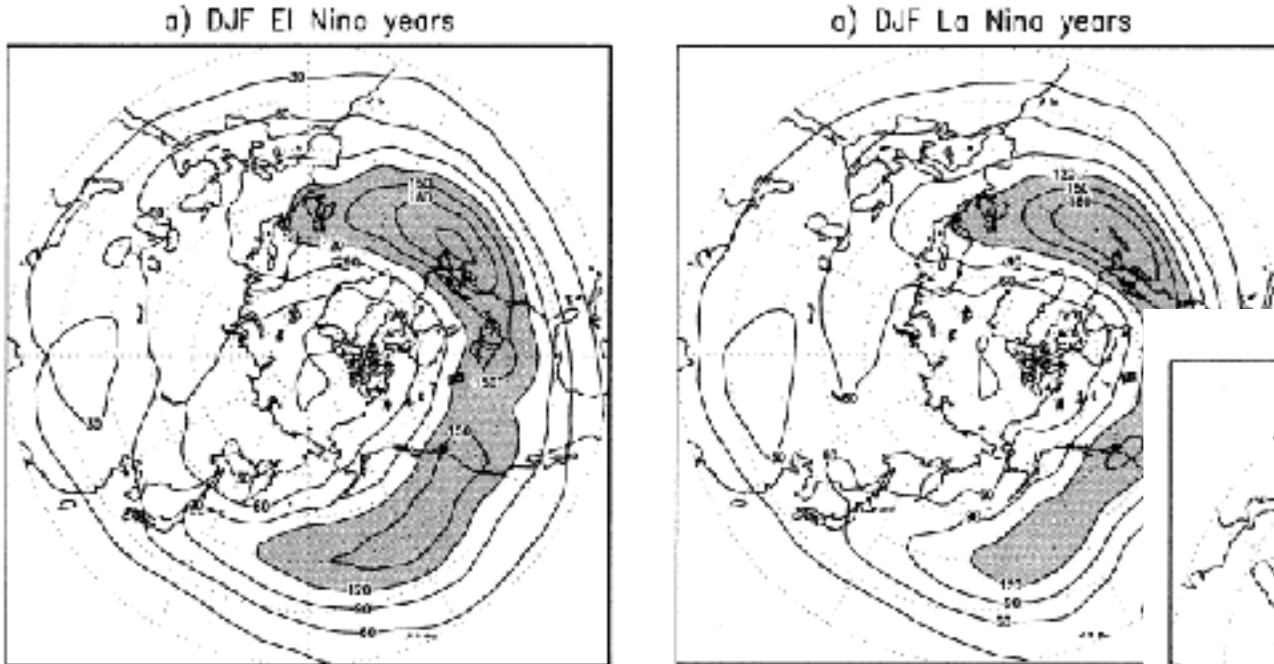

The Pacific storm track shifts equatorward and downstream during El Nino years, which is considered in response to the local enhancement of the Hadley Cell.

from Chang et al, JC, 2002

Observed features

- Decadal variation

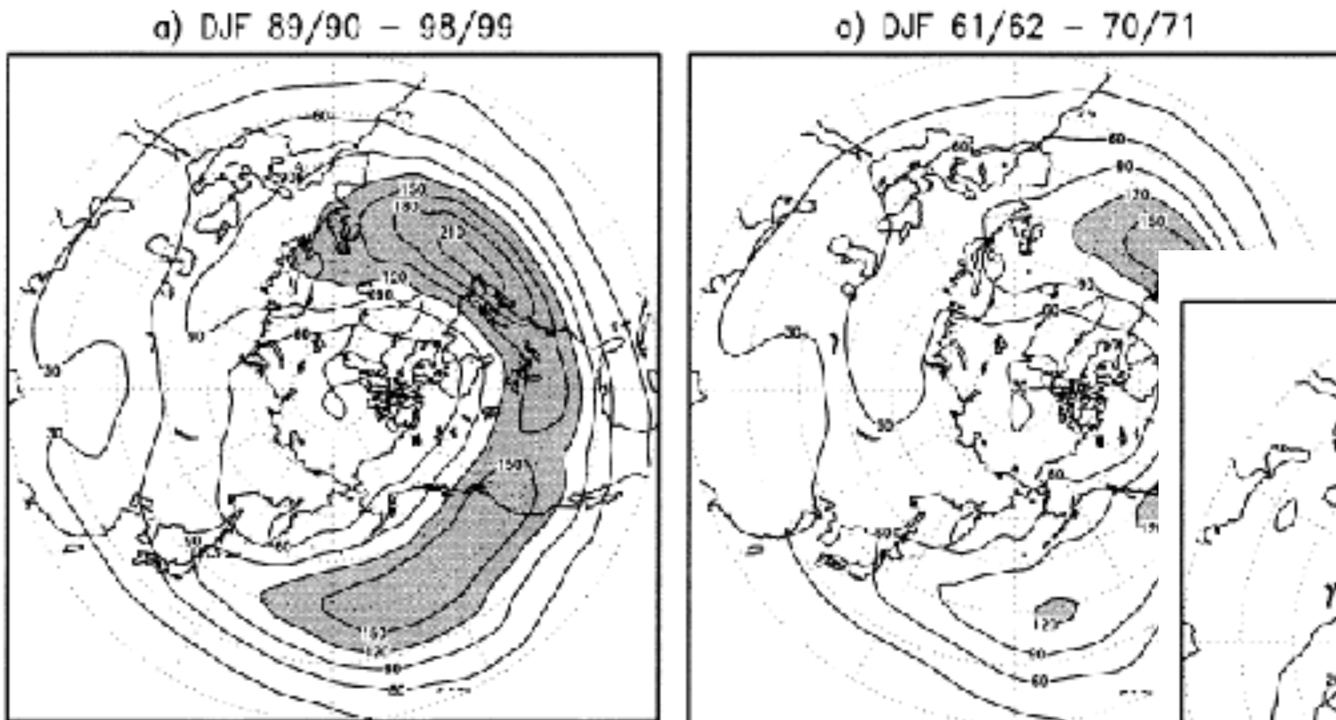

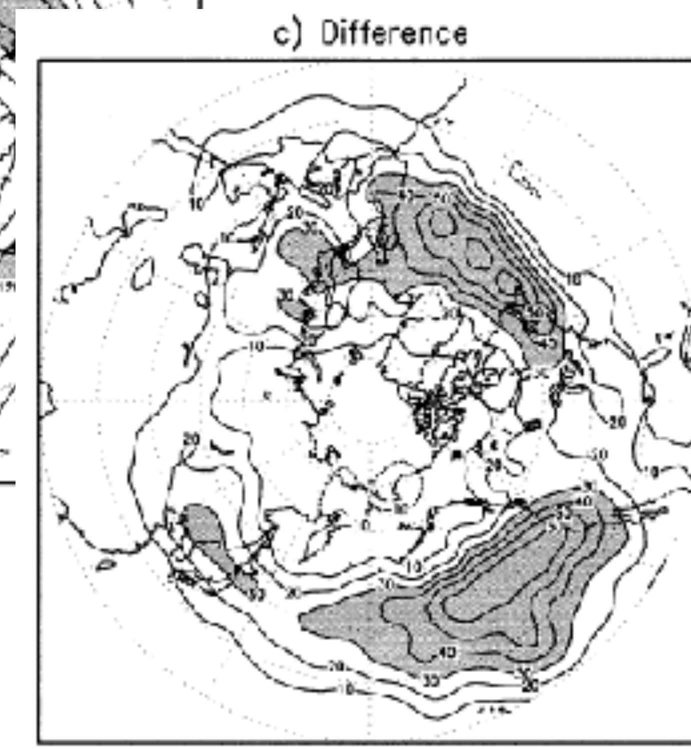

Stronger storm tracks during 1990s in both storm tracks, which shows significant interdecadal variabilities.

from Chang et al, JC, 2002

Observed features

- Summary:
  - Structure: zonally located in the north Pacific and north Atlantic, with the mean flow baroclinicity, jet, eddy activity, eddy heat and momentum flux in different zonal distribution.
  - Seasonal variation: different variations between the Pacific and Atlantic storm tracks; for the Pacific storm zone, mid-winter minimum observed.
  - Inter-annual variation: Pacific storm track shifts equatorward and downstream during El Nino years.
  - Decadal variation: variations in intensity occur in both storm zones, with the storm tracks in the 1990s stronger than in the 1960s.

Outline

- Observed features
  - from two basic approaches
  - seasonal variation
  - inter-annual, decadal variations
- Storm track dynamics
  - Baroclinic eddy life cycle
  - Transient eddy energy budget
- Summary and discussion

Storm track dynamics

- from the baroclinic eddy life cycle

- Eddies' development with idealized GCM:

Small amplitude perturbations

Finite amplitude perturbations

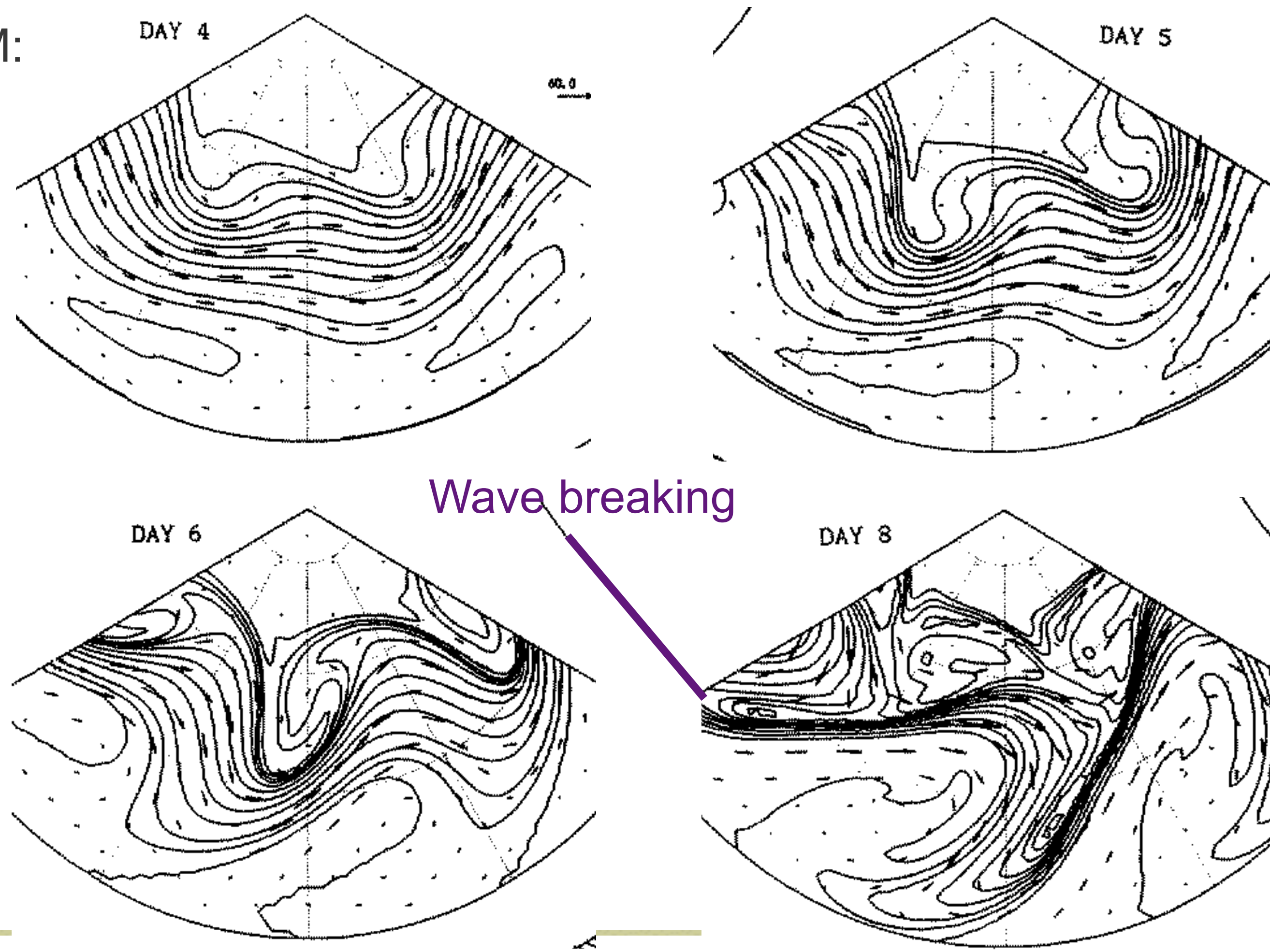

(Thorncroft et al, 1993, Q.J.R.)

Storm track dynamics
- from the baroclinic eddy life cycle

$$\frac{\partial P_M}{\partial t}$$

$< P_{\mathrm{E}}, P_{\mathrm{M}} >$

$c_p \Gamma [v^* T^*] \frac{\partial [T]}{\partial y}$

$$\frac{\partial P_E}{\partial t}$$

$< P_{\mathrm{E}}, K_{\mathrm{E}} >$

$R \frac{[\omega^* T^*]}{p}$

$$\frac{\partial K_E}{\partial t}$$

$< K_{\mathrm{E}}, K_{\mathrm{M}} >$

$\frac{\partial [u]}{\partial y} [u^* v^*]$

$$\frac{\partial K_M}{\partial t}$$

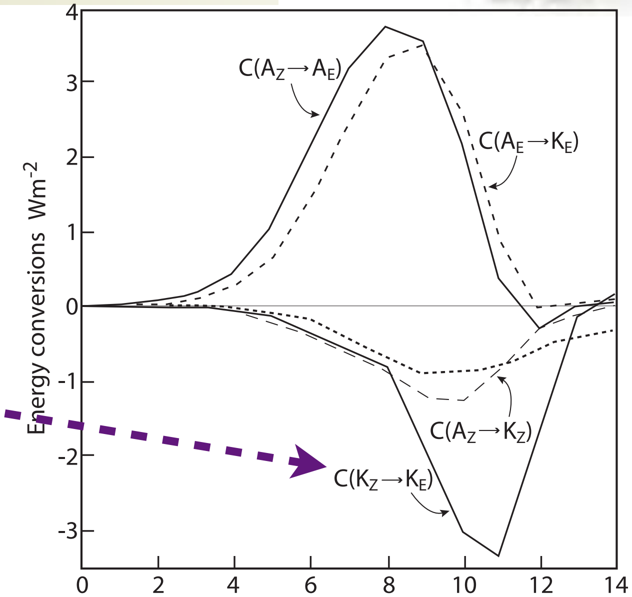

Numerical results from
Simmons and Hoskins, 1978, JAS

Baroclinic eddy life cycle in **time**:

Relatively small amplitude pert. → Baroclinic growth → Finite amplitude perturbation → Barotropic decay

Storm track dynamics

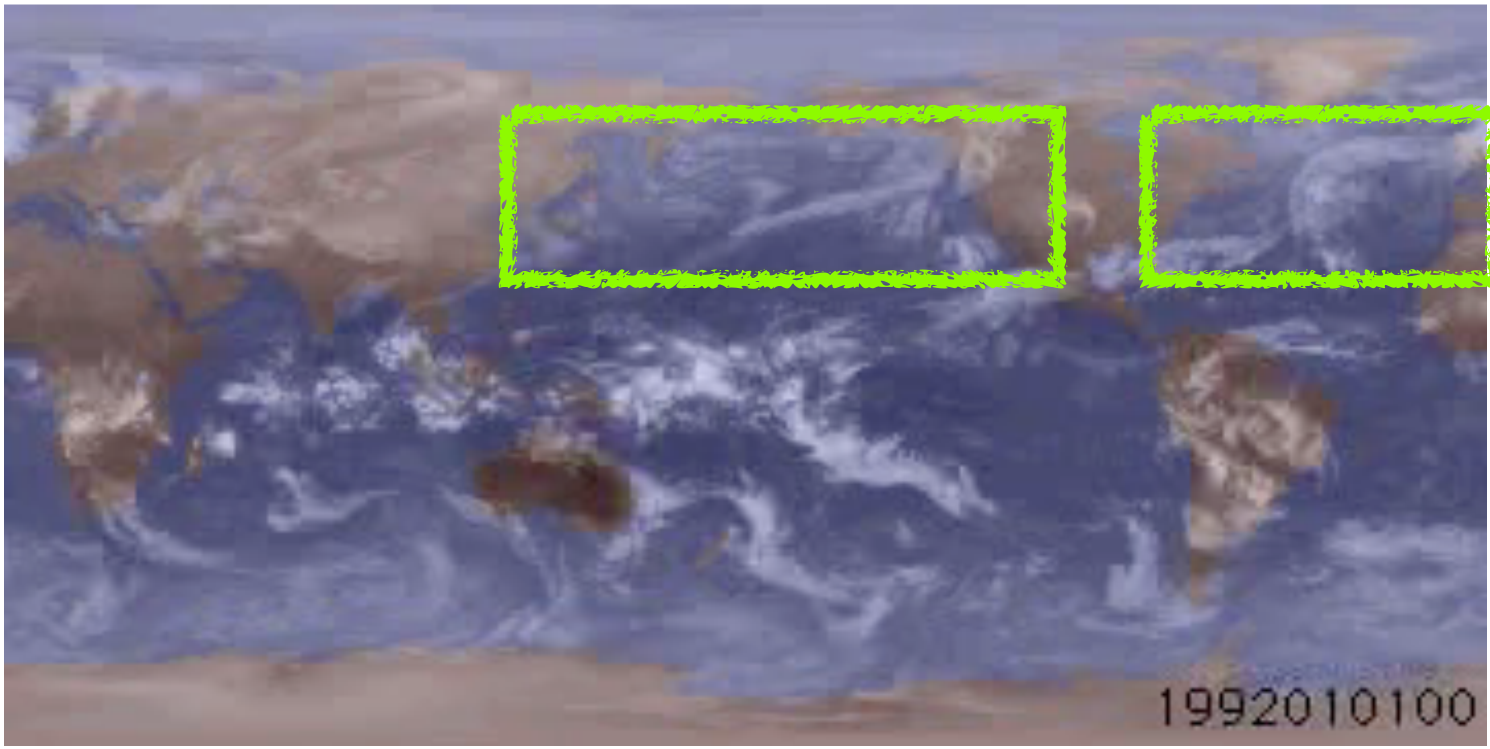

Storm track dynamics

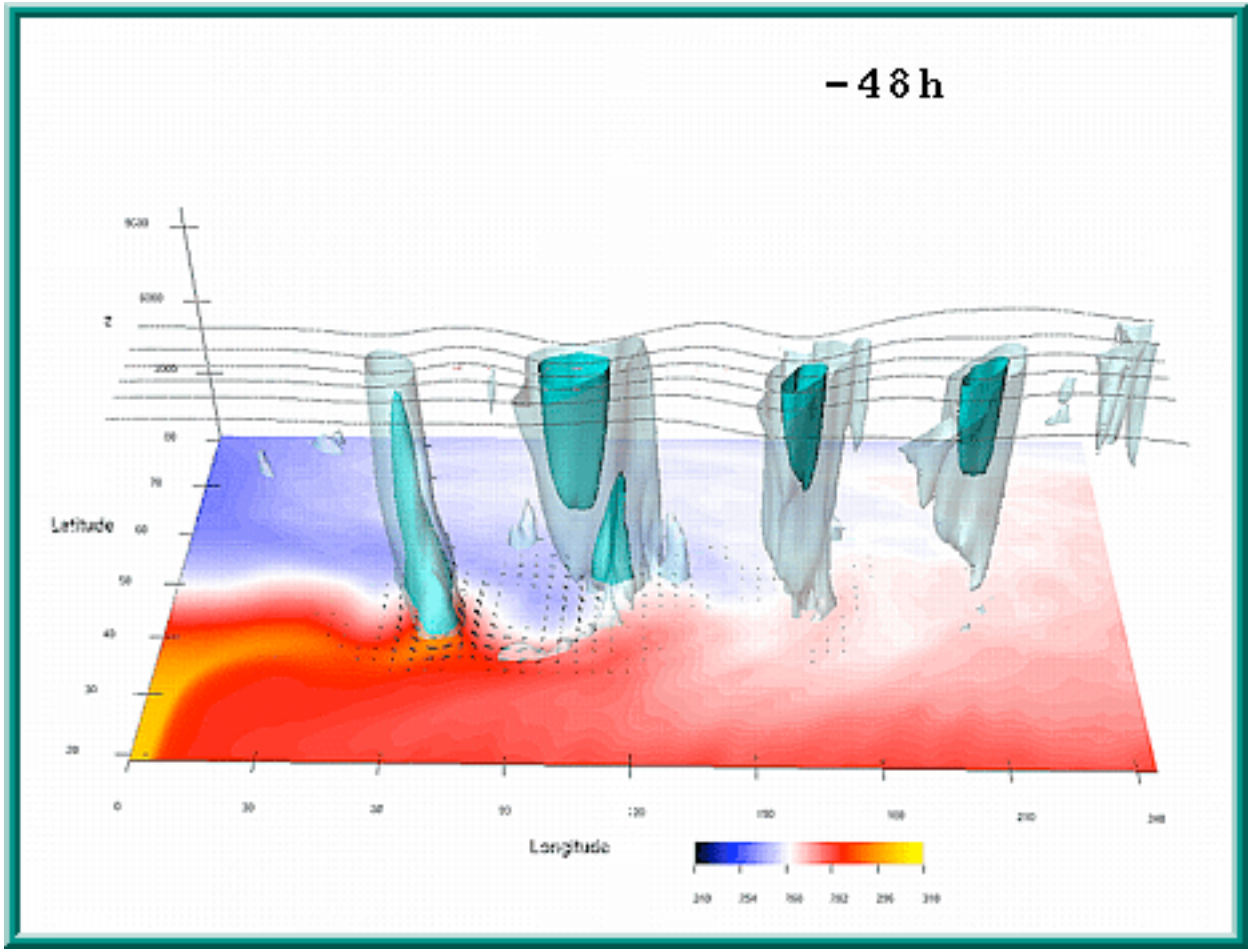

Numerical simulation from Orlanski

Storm track dynamics

- from the baroclinic eddy life cycle

Baroclinic eddy life cycle in **time**:

Relatively small amplitude pert. → Baroclinic growth → Finite amplitude perturbation → Barotropic decay

Storm track structure can heuristically equate with an eddy life cycle in **space**:

Upstream end: perturbations are introduced and begin develop. (entrance region)

develop in space and time

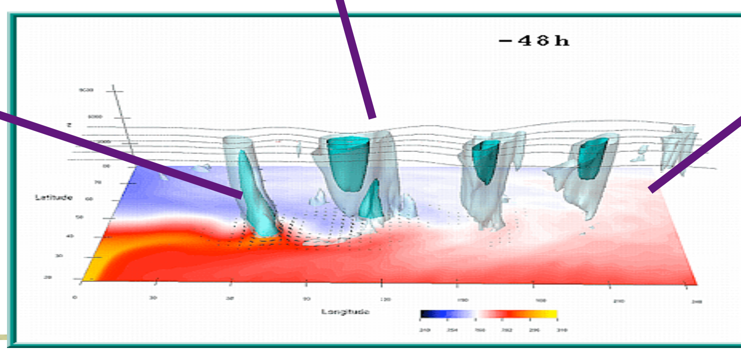

Downstream end: decay stage of the eddy life cycle. (exit region)

Storm track dynamics

- Transient eddy energy budget

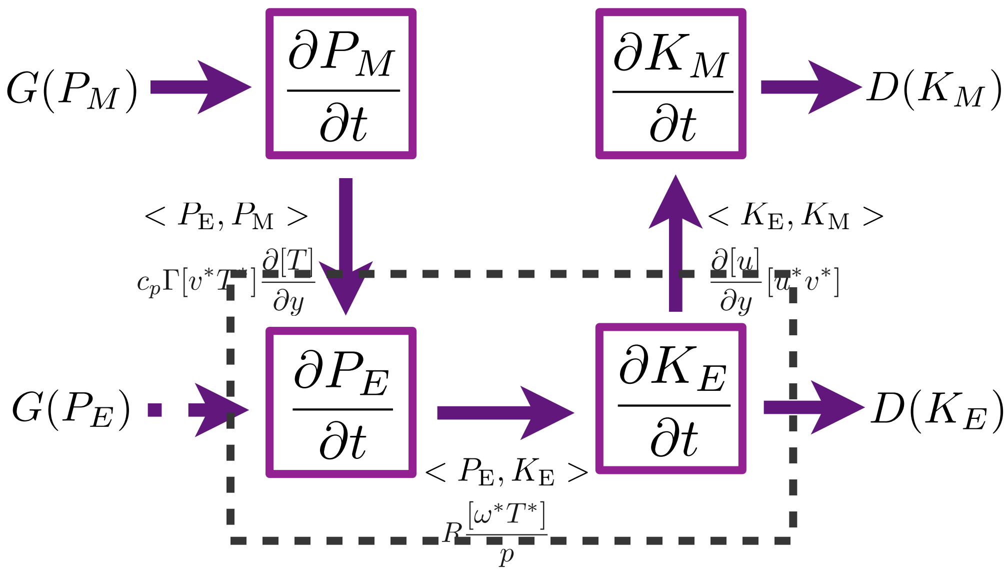

Total eddy energy

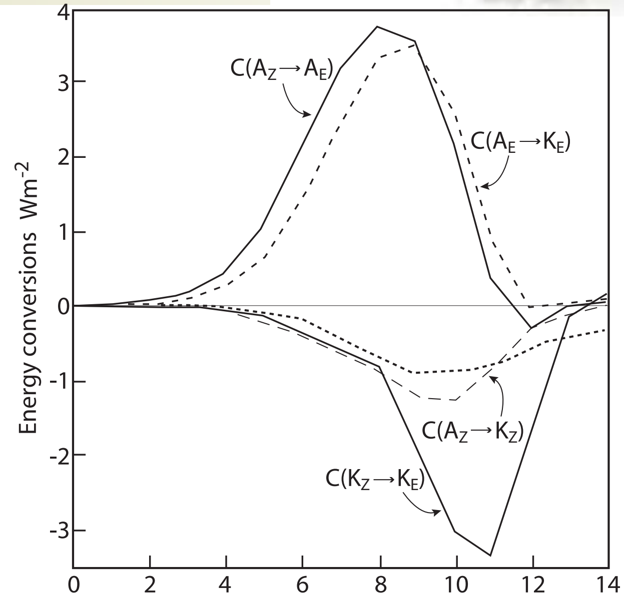

Numerical results from
Simmons and Hoskins, 1978, JAS

For storm tracks, define a **total transient eddy energy**:

$$E = K_{\mathrm{TE}} + P_{\mathrm{TE}} = \frac{1}{2}\overline{(u'^2 + v'^2)} + \frac{c_p}{2}\Gamma\overline{(T'^2)} = \frac{1}{2}\overline{(u'^2 + v'^2)} - \frac{\alpha_m}{2\theta_m}\frac{\overline{\theta'^2}}{\partial\theta_s/\partial p}$$

$A' = A - \overline{A}$, "*m*" denotes mean quantities, $\alpha = 1/\rho$

Storm track dynamics

- Transient eddy energy budget

For storm tracks, define a **total transient eddy energy**:

$$E = K_{\mathrm{TE}} + P_{\mathrm{TE}} = \frac{1}{2}\overline{(u'^2 + v'^2)} + \frac{c_p}{2}\Gamma\overline{(T'^2)} = \frac{1}{2}\overline{(u'^2 + v'^2)} - \frac{\alpha_m}{2\theta_m}\frac{\overline{\theta'^2}}{\partial\theta_s/\partial p}$$

Transient eddy energy budget:

$$\frac{\partial E}{\partial t} = \nabla\cdot\overline{(\mathbf{v}E + \mathbf{v}'_{\mathbf{a}}\phi')} + \frac{\alpha_m}{\theta_m}\frac{\overline{\mathbf{v}'\theta'}}{\partial\theta_s/\partial p}\cdot\nabla\theta - \overline{\mathbf{v}'\cdot(\mathbf{v}'\cdot\nabla)V_m} - \mathrm{diss} + \mathrm{diab}$$

advective energy flux	baroclinic generation	barotropic conversion	$D(K_E)$	$G(P_E)$

Storm track dynamics

- Transient eddy energy budget

a) Total eddy energy   b) Eddy kinetic energy

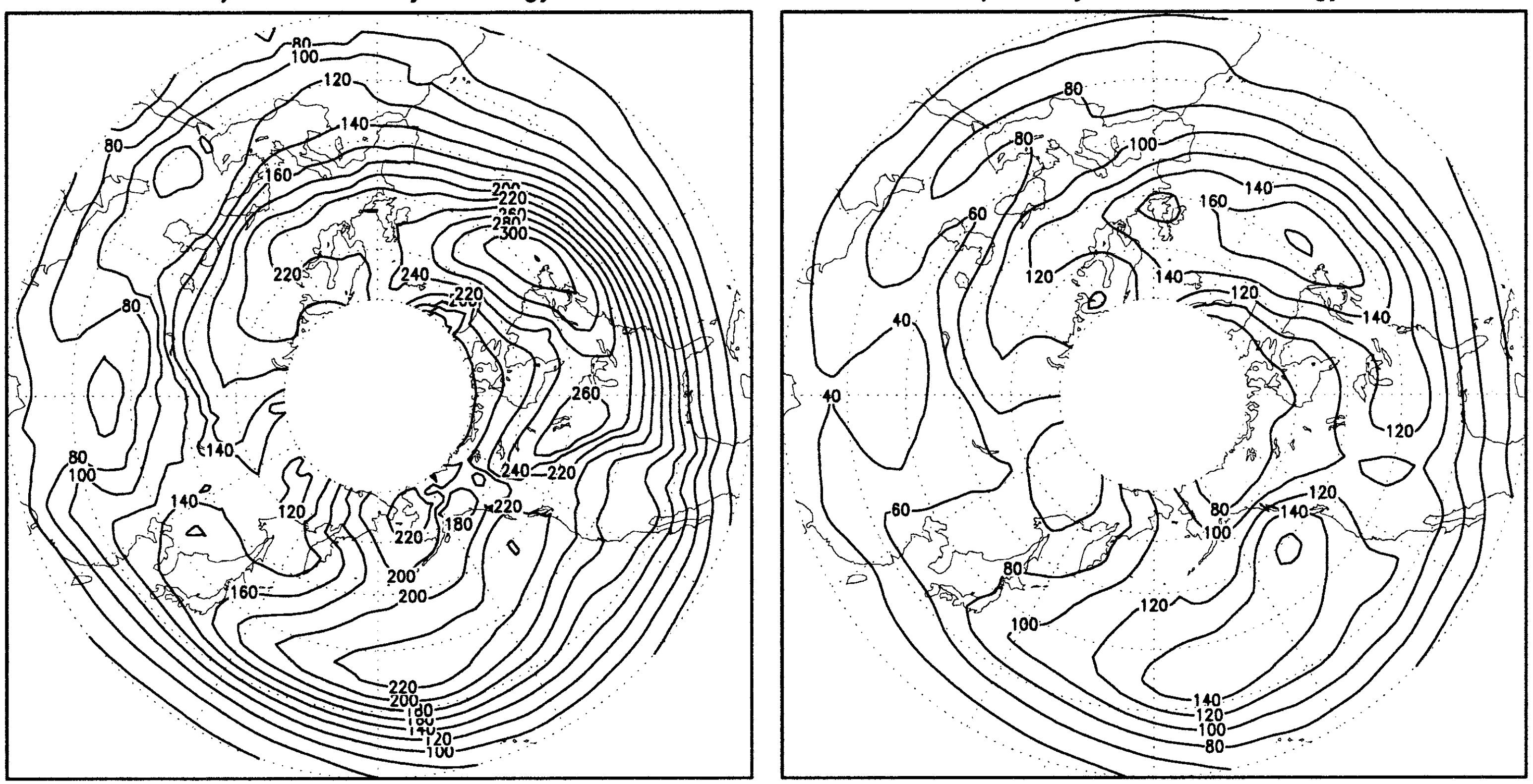

from Chang et al, JC, 2002

Storm track dynamics

- Transient eddy energy budget

c) baroclinic conversion

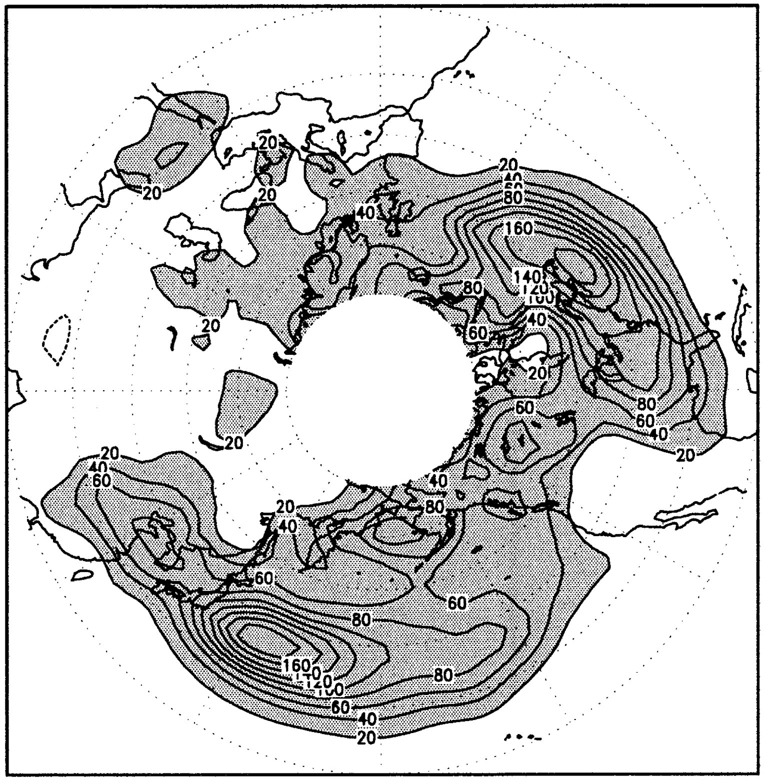

d) barotropic conversion

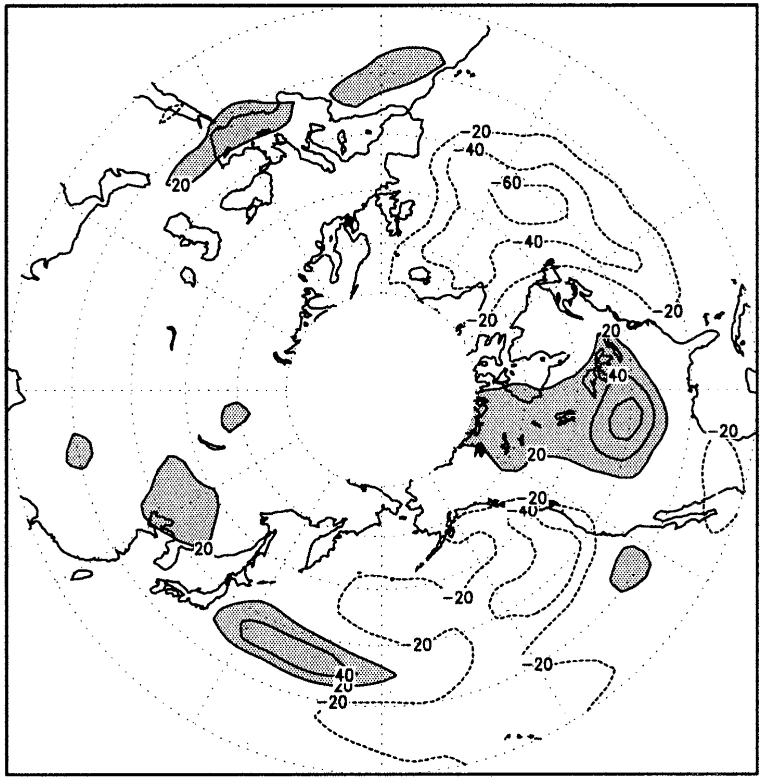

Located upstream

Positive over the entrance region
negative over the exit region

from Chang et al, JC, 2002

Storm track dynamics

- Transient eddy energy budget

e) energy flux f) mechanical dissipation

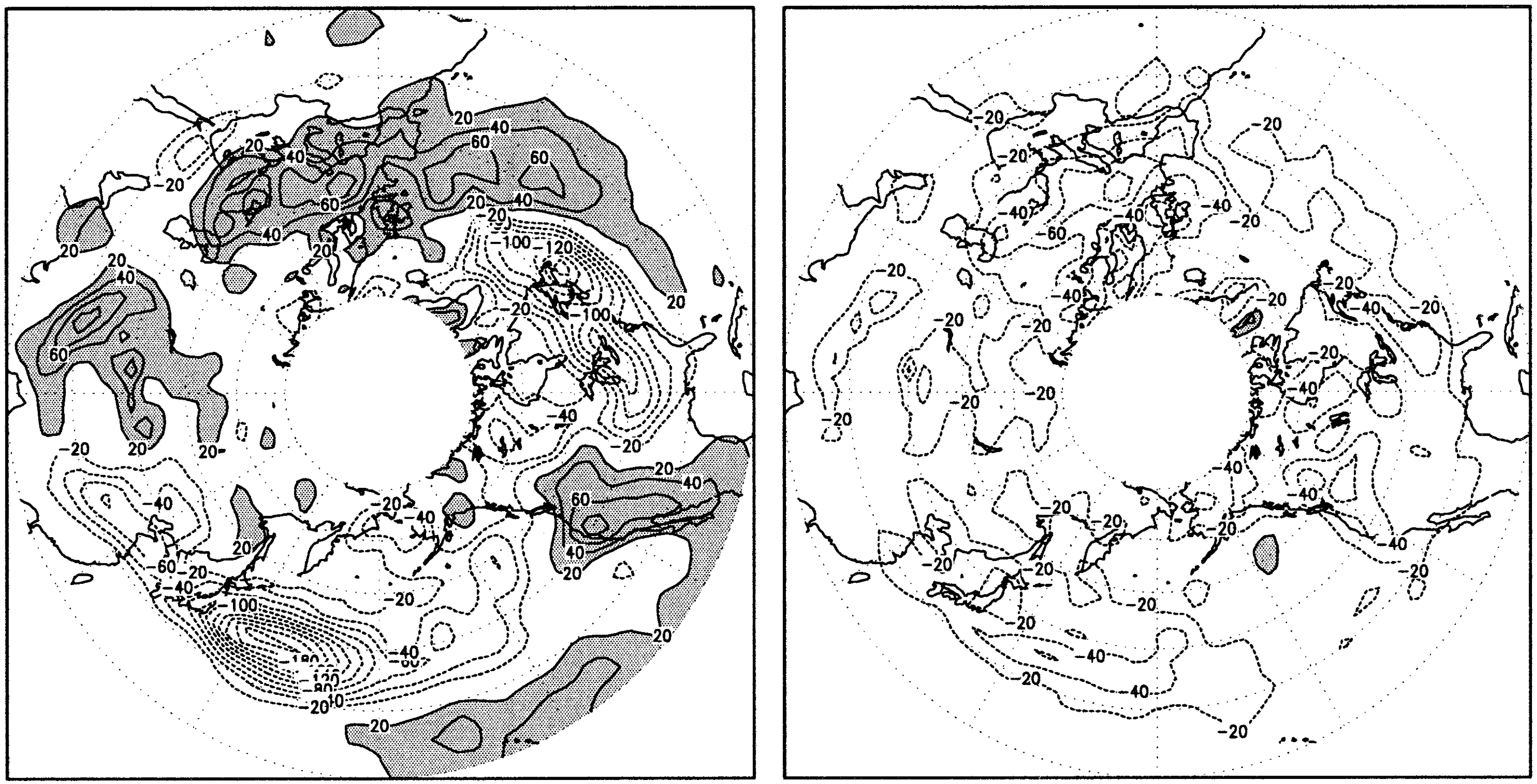

energy sink

from Chang et al, JC, 2002

Storm track dynamics

- Transient eddy energy budget

The role of energy flux: **redistribute** energy from the region where it is generated to downstream regions, **extending** storm track in the zonal direction.

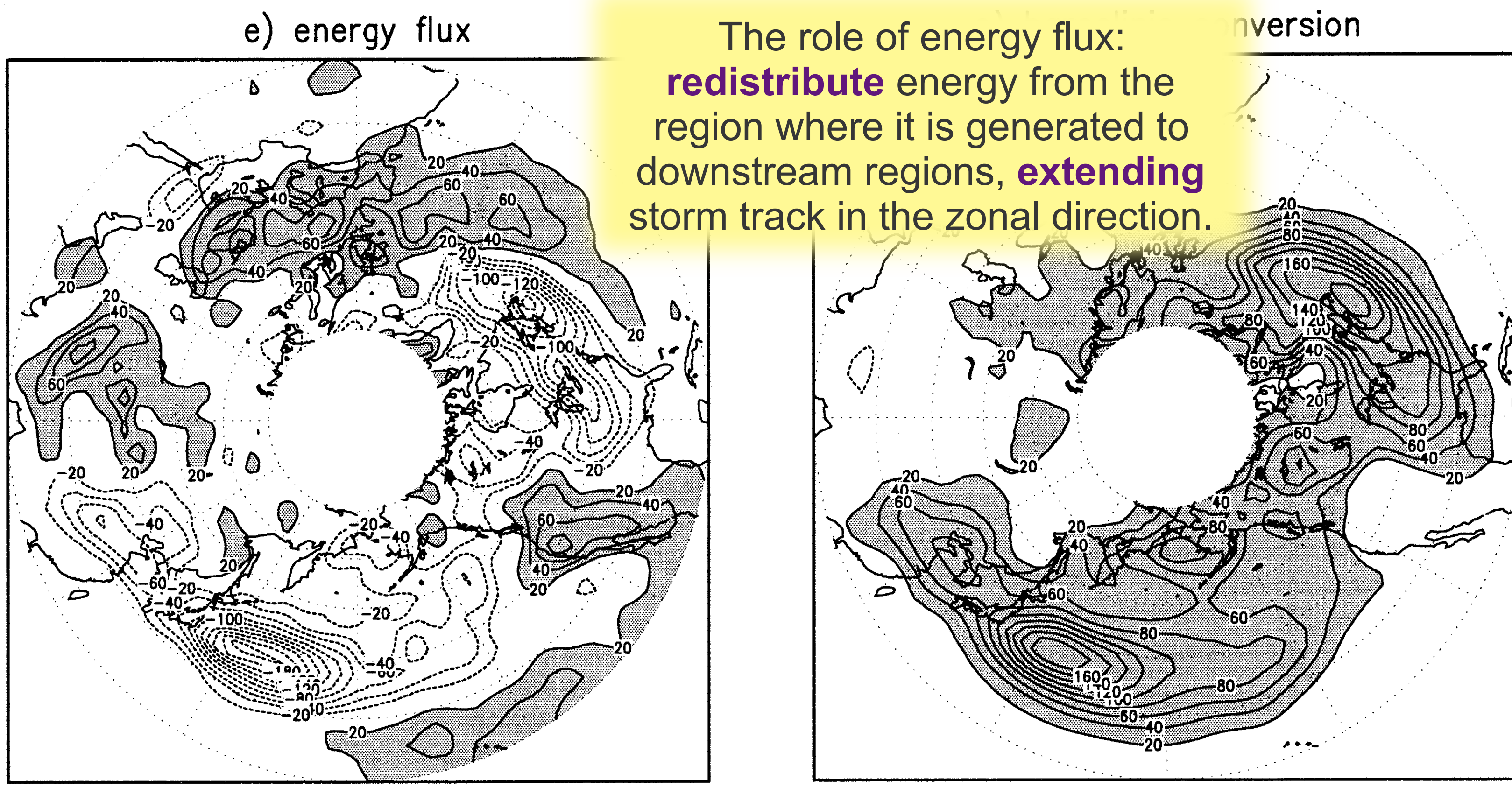

Strongly compensate the baroclinic conversion term in the entrance region.

from Chang et al, JC, 2002

Storm track dynamics
- Transient eddy energy budget

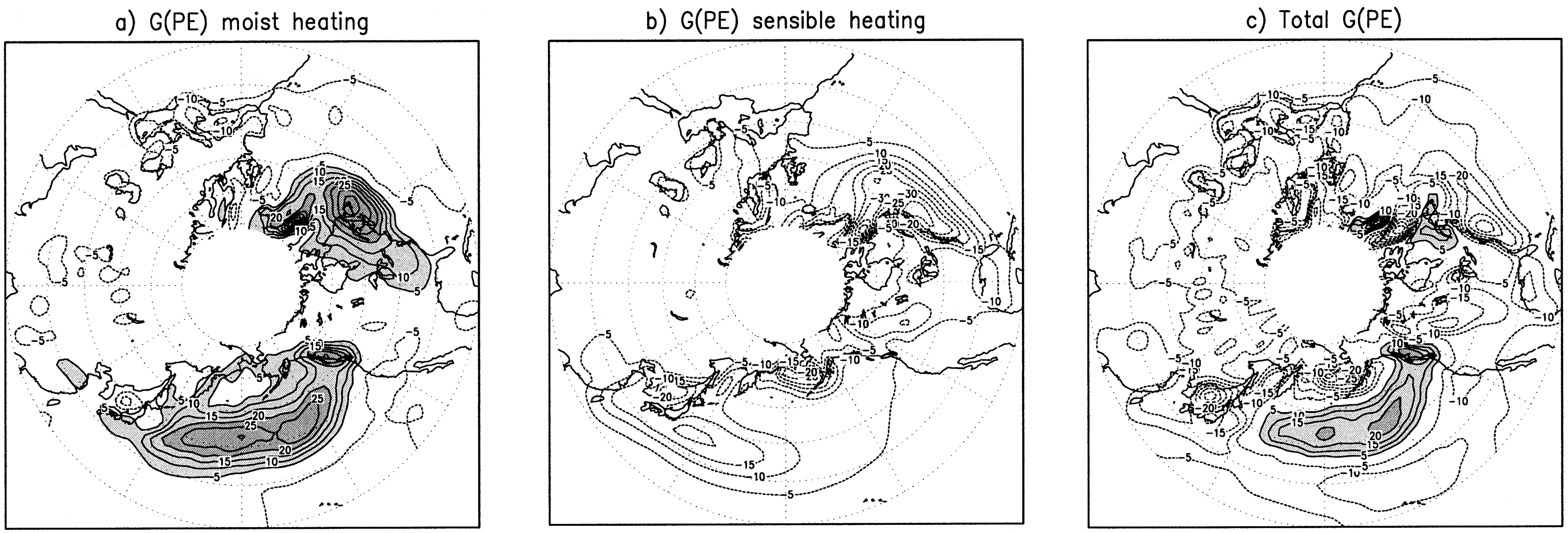

Moist heating: strong along the storm tracks, with the maximum generation rate over the storm track entrance region. (large-scale condensation dominant)

Sensible heating: a strongly negative contribution along the continental east coasts.

Total effect: difference between Pacific and Atlantic region. In the mid and exit regions of **Pacific** storm track, latent heating dominant and enhancing the eddy energy; in the **Atlantic** region, sensible heating dominant.

from Chang et al, JC, 2002

Discussions

- Though the structure of the storm tracks can be partially understood from the view of baroclinic energy cycle occurring in space, many questions are left:
  - Structure: a (causal) relationship between the variability eddies and that of the background flow; the feedbacks between storm track anomalies and the slowly varying planetary-scale flow? e.g. what determines how far downstream of the region of the max baroclinicity the storm tracks extend? Whether the storm track properties can be solely determined by the mean flow? The group propagation of storms...
  - Seasonal variation: the reason of mid-winter minimum?
  - Inter-annual variation: the detailed mechanism of Pacific storm track shift between El nino and La nina years?
  - Decadal variation: the reason for decadal variation and its relation to the global warming?
  - Simulations: AGCM and storm track model

Reference

Chang E.K.M., Lee S., and Swanson K. (2002). Storm track dynamics. J. Climate, 15, 2163–2183.

Hoskins B.J. and Hodges K.I. (2002). New perspectives on the Northern Hemisphere winter storm tracks. J. Atmos. Sci., 59, 1041–1061.

Vallis, G. K. and Gerber, E. P. 2008. Local and Hemispheric Dynamics of the North Atlantic Oscillation, Annular Patterns and the Zonal Index. *Dyn. Atmos. Oceans,*44, 184-212.

Penny, S., Roe, G. H., and Battisti, D. S., The source of the midwinter suppression in storminess over the North Pacific, *J. Climate* , 2010.